JACS
JOURNAL OF THE AMERICAN CHEMICAL SOCIETY
Article
pubs.acs.org/JACS

Quantitative Understanding of Guest Binding Enables the Design of Complex Host–Guest Behavior

Maarten M. J. Smulders,*[,†,‡] Salvatore Zarra,[‡] and Jonathan R. Nitschke*

Department of Chemistry, University of Cambridge, Lensfield Road, Cambridge CB2 1EW, United Kingdom

Supporting Information

ABSTRACT: We report a detailed binding study addressing both the thermodynamics and kinetics of binding of a large set of guest molecules with widely varying properties to a water-soluble M_4L_6 metal–organic host. The effects of different guest properties upon the binding strength and kinetics were elucidated by a systematic analysis of the binding data through principal component analysis, thus allowing structure–property relationships to be determined. These insights enabled us to design more complex encapsulation sequences in which multiple guests that were added simultaneously were bound and released by the host in a time-dependent manner, thus allowing multiple states of the system to be accessed sequentially. Moreover, by inclusion of the pH-sensitive guest pyridine, we were able to further extend our control over the binding by creating a reversible pH-controlled three-guest sequential binding cycle.

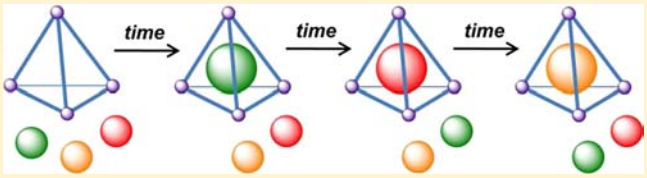

INTRODUCTION

The advent of supramolecular chemistry, defined by Lehn as "*chemistry beyond the molecule*",[1] has created new avenues for chemists to explore molecular self-assembly and self-organization.[2] Drawing inspiration from nature, scientists have begun to create synthetic systems from which complex behavior emerges,[3] thus leading to the development of the field of systems chemistry.[4] Rigorous quantitative physical-organic understanding provides the key to deciphering complexity based upon underlying principles, thus allowing for the bottom-up design of complex chemical systems.[5]

Supramolecular metal–organic polyhedral complexes[6] have proven useful in a range of different applications, including guest binding and separation,[7] cavity-controlled catalysis,[6a,8] generation of unusual reaction products,[9] and stabilization of reactive intermediates.[10] The development of these applications, as well as the invention of new ones, is grounded upon detailed, quantitative insights into the binding of specific guests into the cavities of these polyhedral complexes.[7a,11] Moreover, a detailed physical-organic understanding is essential to the development of more complex host–guest behavior in such systems, such as systems in which the binding of multiple guests can be modulated (in a time-dependent manner, as demonstrated in the present work) or a first binding event affects a second event (allostery).

However, to date, most reported binding studies have been limited to a relatively small set of structurally similar guests (if not a single guest) and tended to focus on the thermodynamics of binding; the kinetics of binding has attracted less interest, except in a few cases. Examples of these include the kinetic studies by Raymond's group on the host–guest behavior of a $[Ga_4L_6]^{12-}$ capsule, revealing a nondissociative guest exchange mechanism,[12] and Rebek and co-workers' report on how the guest-binding kinetics and strength of an organic host vary with the length of a series of linear alkane guests.[13]

Herein we present a study of a set of guest molecules with widely varying properties and report the strength as well as the kinetics of their binding to a M_4L_6-type metal–organic host (Scheme 1). These detailed results allowed the determination of "structure–property relationships", in which the strength and kinetics of binding can be related to the molecular descriptors used to characterize the guest molecules. The understanding thus gained served as a foundation for the realization of "complex" systems, in which multiple guests were sequentially bound by the host in a controlled time-dependent manner.

We previously reported the synthesis of the anionic Fe_4L_6 metal–organic capsule **1** (Scheme 1)[14] and showed how

Scheme 1. Schematic Representation of the Guest Binding Process in Cage 1[a]

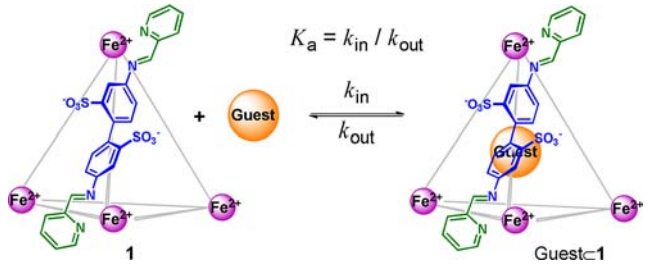

[a]The binding constant K_a is the ratio of the rate constant for guest uptake (k_{in}) to that for guest release (k_{out}).

Received: February 27, 2013
Published: April 1, 2013

 © 2013 American Chemical Society dx.doi.org/10.1021/ja402084x | J. Am. Chem. Soc. 2013, 135, 7039–7046

various guests could be encapsulated inside its cavity, leading to different applications: stabilization of pyrophoric P_4;[10c] sequestration of the most potent greenhouse gas, SF_6;[7a] and supramolecular control over Diels–Alder reactivity.[10a] We also recently reported a qualitative study of the binding properties of the analogous Co_4L_6 and Ni_4L_6 cages.[15]

Although we observed the binding of various hydrophobic guests in the cavity of **1**, such as benzene, cyclohexane, and cyclopentane, binding strengths for only two guests have been reported to date: SF_6 (K_a = 1.3 × 10^4 M^{-1})[7a] and furan (K_a = 8.3 × 10^3 M^{-1}).[10a]

A practical obstacle in determining the binding strength of guests in our system is the limited water solubility of the hydrophobic guests that were observed to bind. To overcome this limitation, we performed competitive binding experiments, a method successfully employed by Raymond and co-workers.[16] In addition, we investigated less hydrophobic (i.e., more water-soluble) guests, for which the determination of K_a by NMR titration was feasible. In the work reported here, we examined a set of 24 guests, for which the observed binding constants ranged from less than 10 M^{-1} to nearly 10^5 M^{-1}.

To date, investigations on the kinetics of guest uptake into **1** have been limited to the determination of the rate constant for cyclohexane encapsulation.[17] A more complete investigation of the uptake kinetics for a wide range of guests, with the aim of understanding the underlying physical explanations of this phenomenon, is also presented in this report.

Finally, we discuss herein the guest properties (as quantified by their molecular descriptors) that have the biggest influence on the guest-binding strength and guest-uptake rate, basing our considerations upon principal component analysis (PCA). PCA is a mathematical method used to reduce the dimensionality of a data set while retaining the variability in the data, and it provides a graphical representation of the correlations that exist in the data set. More detailed information on PCA, including an accessible mathematical explanation of the method, can be found elsewhere.[18] One of the fields in which PCA has recently been fruitfully applied is in the assembly of chemical sensor arrays.[18,19]

The kinetic and thermodynamic insights gained through our quantitative studies were essential to design the more "complex" systems reported herein, in which multiple guests interact with the host in a time-dependent manner, thus allowing multiple states of the system to be probed.

RESULTS AND DISCUSSION

Thermodynamic Studies of Guest Uptake. We first investigated guest-binding strengths. To explore the scope of binding, we considered not only hydrophobic guests but also more water-soluble guests (Table 1). On the basis of their water solubilities and binding strengths, the guests were split into three different categories, each of which required the use of a different strategy to determine the K_a values, as detailed below.

The first category of guests had water solubilities exceeding 1.0 × 10^{-2} M, allowing conventional ^{1}H NMR titrations to be performed. The degree of guest binding to cage **1** was monitored as progressively more of the guest was added to a solution of the host, whose concentration was kept constant [typical host concentrations were in the range (1–2) × 10^{-3} M]. As guest exchange was slow on the NMR time scale, it was possible to observe two sets of resonances corresponding to either free **1** or to the cage with a guest inside. Integration of the respective ^{1}H resonances allowed a straightforward determination of the degree of binding. Nonlinear curve fitting of the data to a 1:1 binding model[20] yielded the binding constants (Figure 1 and Table 1). This method allowed determination of the binding constant for benzene, K_a = (3.0 ± 0.6) × 10^3 M^{-1}, which served as the basis for many others, as detailed below.

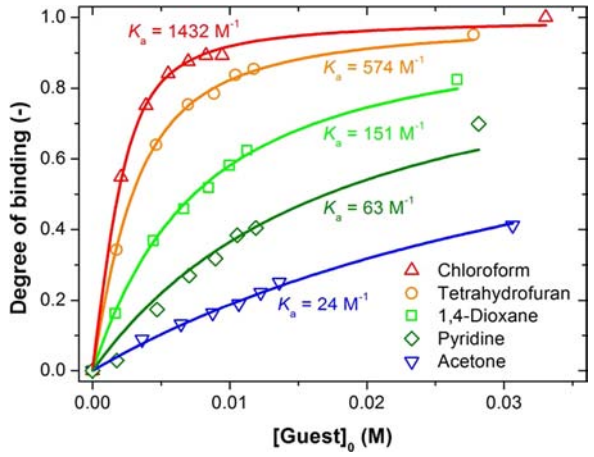

Figure 1. Representative binding isotherms for five of the studied guests: chloroform, tetrahydrofuran, 1,4-dioxane, pyridine, and acetone. $[\mathbf{1}]_0$ = 2.3 × 10^{-3} M. Binding isotherms for all of the guests and details of the data fitting are provided in the Supporting Information.

The second category of guests comprised hydrophobic guests observed to bind weakly. Their low water solubilities prevented direct determination of their binding constants via ^{1}H NMR titration. For this class of guests, we prepared cage solutions and added enough of the guest to saturate the aqueous solution. Under these conditions, the free guest concentration is equal to the maximum water solubility of the guest (S_{MAX}).[21] The stability constant describing the equilibrium between the host (H), guest (G), and host–guest adduct (HG) is given by

$$K_a = \frac{[HG]}{[H][G]} = \frac{[HG]}{[H]} \times \frac{1}{S_{MAX}} \quad (1)$$

Therefore, under guest-saturated conditions, it was possible to calculate the binding constant directly by measurement of the HG/H ratio through integration of the corresponding ^{1}H NMR resonances.

For the third category of guests, which included hydrophobic guests that were found to bind strongly to host **1**, a methodology similar to that for the second class of guests was employed. However, when the aqueous solution was saturated with these guests, because of their strong binding, no empty host was observed by NMR spectroscopy. Consequently, eq 1 could not be used to calculate the binding constant. To circumvent this practical problem, we prepared a solution saturated with both benzene (G_1)[22] and the second guest of interest (G_2) in the presence of cage **1**. Under these conditions, an equilibrium between the two host–guest adducts HG_1 and HG_2 is established:

$$HG_1 + G_2 \rightleftarrows HG_2 + G_1$$

For this equilibrium, the corresponding equilibrium constant (K_{rel}) is given by

dx.doi.org/10.1021/ja402084x | J. Am. Chem. Soc. 2013, 135, 7039–7046

Table 1. Overview of the Investigated Guests, Relevant Molecular Descriptors, and Corresponding Binding Constants (K_a) and Rate Constants for Guest Uptake (k_{in}); All Data Were Either Calculated or Measured at Room Temperature (298 K)

guest	V (Å^3)[a]	Ω_A[a]	S_{MAX} (M)[b]	log$P$[c]	μ (D)[c]	K_a (M^{-1})	k_{in} (M^{-1} s^{-1})
acetone	72.74	0.05329	misc.[d]	−0.24	2.88	24.1 ± 0.4	1.4 ± 0.2
pyridine	92.85	0.06258	misc.	0.65	2.215	63 ± 5	(7.0 ± 0.4) × 10^{-2}
pyridazine	85.96	0.06261	misc.	−0.72	4.22	3 (estimated)[e]	not measured[f]
pyrimidine	86.45	0.06256	misc.	−0.40	2.334	33 ± 1	(1.14 ± 0.04) × 10^{-1}
pyrazine	86.53	0.06283	misc.	−0.26	0	31 ± 2	(1.25 ± 0.06) × 10^{-1}
tetrahydropyran	102.64	0.04096	0.933	0.95	1.58	(7.4 ± 1.3) × 10^2	(8.7 ± 0.2) × 10^{-4}
1,3-dioxane	93.63	0.04229	0.994	0.18	2.06	(3.3 ± 0.3) × 10^2	(1.2 ± 0.1) × 10^{-3}
1,4-dioxane	93.77	0.04234	misc.	−0.27	0	(1.5 ± 0.1) × 10^2	(1.14 ± 0.06) × 10^{-3}
1,3,5-trioxane	84.41	0.04396	3.22	−0.43	2.08	(5.7 ± 0.1) × 10^2	(5.9 ± 0.3) × 10^{-3}
tetrahydrofuran	85.92	0.04036	misc.	0.46	1.75	(5.7 ± 0.1) × 10^2	(8.3 ± 0.1) × 10^{-3}
furan	77.83	0.06255	0.151	1.34	0.66	(8.3 ± 0.7) × 10^3 [g]	2.1 ± 0.3
CH_2Cl_2	60.83	0.18676	0.234	1.25	1.6	(1.3 ± 0.2) × 10^3	(1.06 ± 0.01) × 10^3
$CHCl_3$	74.68	0.05589	6.76 × 10^{-2}	1.97	1.04	(1.4 ± 0.1) × 10^3	1.57 ± 0.02
CCl_4	88.69	0	4.90 × 10^{-3}	2.83	0	(2.2 ± 0.5) × 10^4	(1.9 ± 0.2) × 10^{-2}
SF_6	73.06	0	n/a[h]	1.68	0	(1.3 ± 0.3) × 10^4 [i]	not measured[j]
methylcyclopentane	113.05	0.07194	5.01 × 10^{-4}	3.37	0	(1.3 ± 0.2) × 10^4	(5.1 ± 0.3) × 10^{-3}
cyclohexane	111.48	0.03989	7.94 × 10^{-4}	3.44	0	(7.1 ± 1.5) × 10^4	(3.52 ± 0.03) × 10^{-3} [k]
methylcyclohexane	148.33	0.06599	1.41 × 10^{-4}	3.61	0	nonbinding	not measured[f]
cycloheptane	145.65	0.03934	3.09 × 10^{-4}	4.00	0	nonbinding	not measured[f]
cyclohexene	108.16	0.03883	2.57 × 10^{-4}	2.86	0.332	(2.1 ± 0.4) × 10^4	(8.9 ± 0.2) × 10^{-3}
1,3-cyclohexadiene	103.77	0.05052	n/a[h]	2.47	0.44	(1.7 ± 0.4) × 10^4	(8.1 ± 0.2) × 10^{-3}
benzene	99.16	0.06250	2.29 × 10^{-2}	2.13	0	(3.0 ± 0.6) × 10^3	(1.58 ± 0.01) × 10^{-1}
fluorobenzene	103.83	0.08936	1.58 × 10^{-2}	2.27	1.6	(6.1 ± 2.4) × 10^2	(2.21 ± 0.01) × 10^{-1}
toluene	134.77	0.08703	6.17 × 10^{-3}	2.73	0.36	nonbinding	not measured[f]

[a]Details on how the volume (V) and asphericity (Ω_A) were calculated are given in the Supporting Information. [b]Maximum solubilities in water, taken from Abraham and Le.[21] [c]Values of the logarithm of the octanol:water partition coefficient (log$P$) and the dipole moment (μ) were taken from the *CRC Handbook of Chemistry and Physics*.[26] [d]Miscible with water. [e]Value determined from a single data point (see the Supporting Information). [f]The value of k_{in} was not determined because the binding constant was too low. [g]Value taken from ref 10a. [h]Value not available in Abraham and Le.[21] [i]Value taken from ref 7a. [j]The value of k_{in} was not determined because the guest is a gas, making it practically difficult to control the guest concentration. [k]Value taken from ref 17.

$$K_{rel} = \frac{[HG_2][G_1]}{[HG_1][G_2]} = \frac{[HG_2]}{[HG_1]} \times \frac{S_{max,1}}{S_{max,2}} = \frac{K_{a,2}}{K_{a,1}} \qquad (2)$$

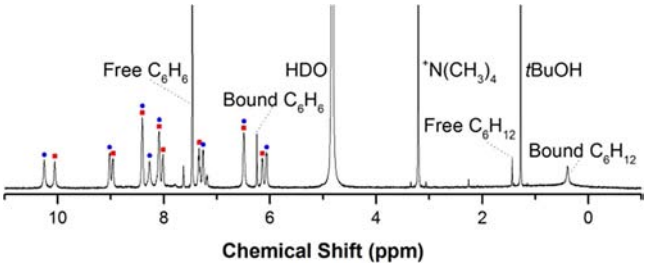

Figure 2. ^{1}H NMR spectrum of cage **1** in the presence of benzene and cyclohexane. Two sets of host peaks can be attributed to benzene⊂**1** (labeled with blue circles) and cyclohexane⊂**1** (labeled with red squares). Signals for both the bound and unbound guests can be seen.

Following equilibration, integration of the ^{1}H NMR signals provided the HG_2/HG_1 ratio. For example, Figure 2 shows the ^{1}H NMR spectrum of host **1** in an aqueous solution saturated with benzene and cyclohexane. Two sets of resonances can be discerned, one for the benzene⊂**1** complex and the other for cyclohexane⊂**1**. The ratio of these two species, after correction for the water solubilities of the respective guests, provides K_{rel}, which is the ratio of the binding constants of the two guests.[16] The binding constant for the second guest, $K_{a,2}$, could be calculated from K_{rel} and $K_{a,1}$, since the binding constant of guest 1 (benzene) is known. Using the three methods outlined above, we were able to determine the values of K_a for the various guests (Table 1).

Elucidation of Factors Governing Binding Strength. The size of the guest is a primary factor in determining whether it will be accommodated into host **1**: above a certain threshold size, no encapsulation was observed to take place.[15] In particular, molecules with seven or more carbon atoms appear to be too large for encapsulation, as evidenced by the absence of new resonances in the ^{1}H NMR spectrum when methylcyclohexane, cycloheptane, or toluene was added to a solution of **1** (see Table 1 and the Supporting Information).

For guests whose volume is below this threshold for encapsulation, we sought to investigate which guest properties favored binding. To address this question, a correlation analysis[23] of different guest molecular descriptors[24] was employed. Four such descriptors were considered: the logarithm of the octanol:water partition coefficient (log$P$), the dipole moment (μ), the molecular volume (V), and the molecular surface area. For all guests, data corresponding to these molecular descriptors together with the logarithm of the binding constant, log K_a, were analyzed by PCA (see the Supporting Information). This approach allowed us to identify the degree of collinearity among the five variables (i.e., the four molecular descriptors and log K_a). In the loading plot, variables that are highly correlated to each other lie either very near each

dx.doi.org/10.1021/ja402084x | J. Am. Chem. Soc. 2013, 135, 7039−7046

other (r value close to 1 in the correlation matrix) or in symmetrical positions relative to each other with respect to the center of the diagram (r value close to −1 in the correlation matrix).[25]

The biplot reported in Figure 3 is the result of the PCA performed on the data considering the five variables (log K_a, log$P$, μ, V, and molecular surface area) for all of the guests that were observed to bind. In the diagram, in which the five-dimensional space has been reduced to a two-dimensional space involving the two principal components, the values of both the variables (the so-called loadings, shown with blue lines) and the components (the so-called scores, shown as red solid circles) for each guest are reported. A close look at the diagram gives an overall picture of which properties make positive contributions and which make negative contributions to the strength of guest binding.

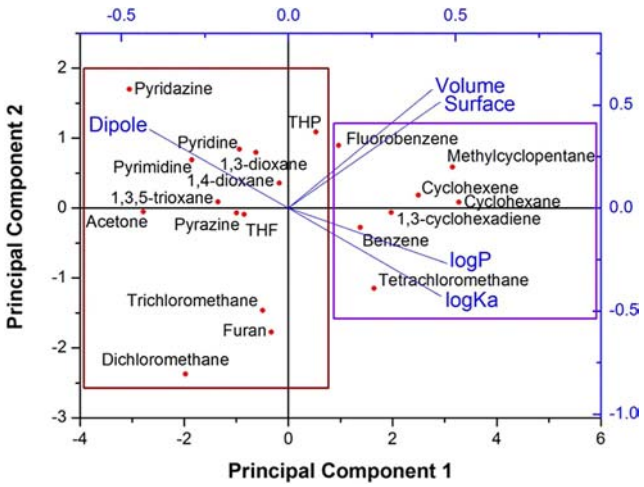

Figure 3. PCA biplot obtained by analyzing five variables (log K_a, log$P$, dipole moment, molecular volume, and molecular surface) for each guest, in which both loadings (blue lines) and scores (red solid circles) are represented. Two subsets of guests can be identified: hydrophobic guests (grouped in the purple rectangle on the right, log $S_{MAX} < -1.5$) and water-soluble guests (grouped in the brown rectangle on the left, log $S_{MAX} > -1.5$).

From analysis of the loading plot (blue lines in Figure 3), it can be concluded that log K_a is highly correlated to μ and log$P$. In particular, higher log$P$ values and lower μ values give higher values of log K_a. Guest dimensions, as described by the molecular surface area and volume, do not have much influence on the binding strength since these variables are not correlated to log K_a. This suggests that the size of the guest, provided it does not exceed an upper limit, is not strongly correlated to the strength of binding.

The guests considered in this binding study are not all part of a single homogeneous class that would include hydrophobic as well as water-soluble and -miscible molecules. This observation emerges from the PCA score plot (red circles in Figure 3), where two subsets of guests can be identified. Guests with a high log$P$ value (i.e., hydrophobic guests, log $S_{MAX} < -1.5$, highlighted with the purple rectangle in Figure 3) have a high log K_a value. This can be rationalized considering that the host's cavity is hydrophobic, so hydrophobic guests prefer being bound to staying in the aqueous phase. On the contrary, water-soluble guests (log $S_{MAX} > -1.5$, highlighted with the brown rectangle in Figure 3) have lower values of log K_a.

Reversible pH-Dependent Guest Binding. The observation that basic pyridine could be encapsulated by host **1** prompted us to study the pH dependence of this binding event. Protonation of pyridine at lower pH would lead to the formation of the pyridinium cation, which we envisioned would not be a guest for host **1**, as in previous work no cationic species were observed to bind within **1**.[7a,14] To investigate this, a solution of host **1** and pyridine in D_2O was prepared ($[\mathbf{1}]_0$ = 2.8 × 10^{-3} M; $[\text{pyridine}]_0$ = 2.0 × 10^{-1} M, degree of encapsulation observed = 93%).

The addition of deuterated trifluoroacetic acid lowered the pD of the solution from 5.4 to 3.9, after which the degree of binding as determined by ^{1}H NMR analysis was only 18% (Figure 4). Further lowering the pD resulted in decomposition of the cage. The pD was subsequently raised in small increments by addition of sodium bicarbonate, and the degree of binding was measured after each addition (Figure 4). Ultimately, at pD 7.3 the degree of binding was again 93%.

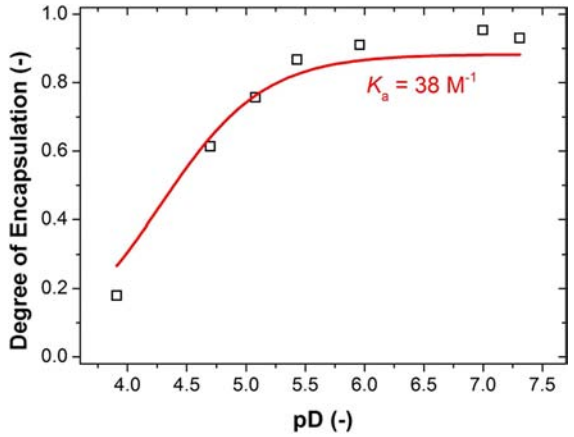

Figure 4. Degree of encapsulation of pyridine as a function of pD. The red line represents a one-parameter fit of the data that yielded K_a for binding of pyridine to **1**. The equation used to fit the data points is given in the Supporting Information.

To analyze further the pD-dependent binding of pyridine we considered the following equilibria to describe the system:

$$\text{Pyridinium} \underset{D^+}{\overset{K_{acid}}{\rightleftharpoons}} \text{Pyridine} \overset{K_a}{\underset{1}{\rightleftharpoons}} \text{Pyridine}\subset\mathbf{1}$$

On the basis of these two equilibria, we derived an analytical expression for the degree of binding of pyridine as a function of pD, assuming that the protonated pyridinium cation cannot bind to host **1** (see the Supporting Information). Although the derived expression has four parameters, three of them are constant throughout the titration: $[H]_0$, $[\text{pyridine}]_0$ and K_{acid}. This leaves a single parameter, K_a, that can be varied to fit the pD-dependent binding data. Nonlinear curve fitting of the data yielded the value $K_a = 38 \pm 5$ M^{-1} (Figure 4), which is in good agreement with the value obtained through direct titration of (63 ± 5 M^{-1}; Table 1). The difference in the values could be explained by a weak affinity for pyridinium, which we assumed to be zero. Hence, controlling the pD allows us to tune the degree of binding of pyridine to host **1** in a reversible manner: we found that lowering the pD could decrease the guest binding from more than 90% to less than 20%.

Kinetic Studies of Guest Uptake. Following the above-described thermodynamic studies on the binding of the various

dx.doi.org/10.1021/ja402084x | J. Am. Chem. Soc. 2013, 135, 7039−7046

guests to host **1**, we set out to study in detail the kinetics of guest uptake by host **1**. The main aim of these kinetic studies was to reveal which guest properties determine the rate of guest encapsulation by **1**. Such insight may help elucidate the factors that govern guest exchange in related host–guest systems, where the exchange between bulk solution and the host cavity takes place through an aperture in a face of the host.[11p,17,27,28]

Of the 24 guests whose thermodynamics of binding were probed (Table 1), the kinetics of the 19 guests that showed binding were also studied. It was possible to determine the rate constants for uptake of both hydrophobic and hydrophilic guests by ^{1}H NMR spectroscopy. For hydrophobic guests, having the lowest water solubilities, a sufficient amount was added to a solution of **1** to ensure that the aqueous phase was saturated with guest. For guests having water solubility exceeding 1.0×10^{-2} M, excess guest (ca. 30 equiv) was employed. Performing the kinetic experiments under these conditions allowed us to treat the guest uptake for both types of guests as a pseudo-first-order process wherein the guest concentration did not change significantly during the course of the experiment.

For most of the guests, it was possible to follow the uptake into host **1** by acquiring 1D ^{1}H NMR spectra at regular intervals (as short as 5 s for the most quickly encapsulated guests, e.g., chloroform). The fraction of empty host **1** was tracked by integrating the peaks corresponding to the free host and the host–guest complex for each spectrum, and this fraction was plotted against time to allow the kinetics to be fit to a first-order rate equation. In the case of weakly binding guests, where empty host **1** was still present in substantial amounts at equilibrium, the fraction of empty host at equilibrium was also considered as a parameter in the data fitting. An apparent first-order rate constant for guest uptake (k_{app}) was determined for each guest investigated with this method (see the Supporting Information). From this rate constant and the guest concentration in the aqueous phase, it was possible to calculate the second-order rate constant for guest uptake (k_{in}). The values of k_{in} are listed in Table 1.

The uptake rates for two guests, acetone and dichloromethane, were too high to be determined as described above; by the time the first spectrum was acquired, the system had already reached equilibrium. Therefore, 2D exchange spectroscopy (EXSY) NMR measurements were used instead (see the Supporting Information). This technique, which has been used to study molecular systems undergoing slow chemical exchange[29] on the NMR time scale (typically between 10^{-2} and 10^2 s^{-1}),[30] allowed the rate constants for magnetization exchange to be determined. Through knowledge of the guest concentrations, the k_{in} values could be calculated.

Elucidation of Factors Governing Guest-Uptake Rate. The guests can be divided into two categories according to their uptake rate constants: slow guests ($k_{in} < 5 \times 10^{-2}$ M^{-1} s^{-1}) and fast guests ($k_{in} > 5 \times 10^{-2}$ M^{-1} s^{-1}). Similarly to the binding constant studies discussed above, different guest properties were considered in order to explain the obtained guest-uptake rate constants. PCA considering seven different variables, including log k_{in}, was performed (see the Supporting Information). Guest size, whose representative variables are molecular volume and molecular surface area, is one of the properties that is strongly correlated with the uptake rate constant (see Figure S6 in the Supporting Information). Plotting log k_{in} versus volume gave a linear relationship (Figure 5A).

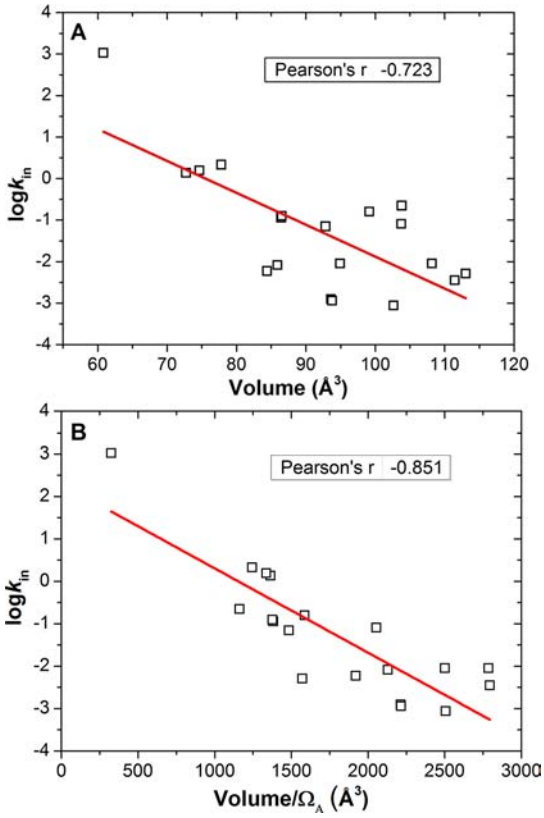

Figure 5. (A) Linear relationship between log k_{in} and guest volume. (B) A better linear relationship was obtained when log k_{in} was plotted against the corrected volume (i.e., volume/Ω_A), as indicated by a higher modulus of the Pearson's correlation coefficient,[33] which is a measure of the linear dependence between two variables. Guests having $\Omega_A = 0$ were not included in the graphs, since the corrected volume calculated for those would be infinity.

As expected, the smallest guests (dichloromethane, acetone, furan, and chloroform) had the highest uptake rate constants, and the two largest guests (cyclohexane and methylcyclopentane) had two of the lowest rate constants (Table 1). For the series of oxygen-containing six-membered rings [i.e., tetrahydropyran (THP), 1,3-dioxane, 1,4-dioxane, and 1,3,5-trioxane], as the volume decreased, the uptake rate constant increased. The same was true across the series of six-membered carbocycles (i.e., cyclohexane, cyclohexene, 1,3-cyclohexadiene, and benzene), for which k_{in} increased as the volume decreased.

The scatter in the plot in Figure 5A suggests that factors other than guest volume may influence the binding kinetics. For example, benzene is encapsulated more rapidly than THP, although the two have nearly equal volumes. A key difference between the two guests appears to be that the aromatic benzene molecule is flat, unlike THP.

In the literature, various molecular descriptors have been used to quantify molecular shape in a meaningful way.[24] These descriptors are often derived from the principal moments of inertia (I_A, I_B, and I_C) of the molecule, which describe the anisotropy of the mass distribution along the three spatial dimensions. These quantities are related to the molecular symmetry and can be combined into an equation to describe the shape of molecules.[31] A parameter relevant to our system is the asphericity (Ω_A), a descriptor for the deviation from a spherical shape, which is defined as[32]

dx.doi.org/10.1021/ja402084x | J. Am. Chem. Soc. 2013, 135, 7039–7046

$$\Omega_A = \frac{1}{2}\cdot\frac{(I_A - I_B)^2 + (I_A - I_C)^2 + (I_B - I_C)^2}{(I_A + I_B + I_C)^2} \quad (3)$$

Values of the asphericity are in the range $0 \le \Omega_A \le 1$: $\Omega_A = 0$ for spherical molecules; $\Omega_A = 1$ for linear molecules; and for disk-shaped molecules ($I_B \approx I_C \gg I_A$), $\Omega_A \approx 0.25$.

To probe the impact of a molecule's asphericity upon the binding kinetics, PCA was again employed (see the Supporting Information). This analysis revealed a positive correlation between log k_{in} and Ω_A, whereby more aspherical molecules (i.e., molecules with Ω_A greater than 0) were observed to exhibit higher rates of uptake. When asphericity was used as a correction factor for guest volume (i.e., when log k_{in} was plotted against volume/Ω_A), a better-quality linear fit was obtained (Figure 5B) than for the uncorrected data (Figure 5A).

In addition to simple considerations of aspect ratio, whereby "thin" molecules would be expected to thread into the cavity of **1** more readily than "thick" ones, the guest's degrees of freedom also have a bearing upon the uptake rate, as reflected in the asphericity. As mentioned above, the flat benzene molecule is taken up more rapidly into the host's cavity than is the chair-shaped THP molecule. The correct orientation of benzene is the only degree of freedom that needs to be fixed in order for it to go through the host's aperture.[11p,17,27] THP also has to adopt a suitable molecular conformation, in addition to a correct orientation, for it to enter host **1**; as a consequence, two degrees of freedom need to be fixed, leading to a higher activation energy barrier for guest uptake. Analogous considerations are also valid for the other flat molecules (pyrimidine, pyrazine, pyridine, and fluorobenzene), which go into the cavity of **1** faster than nonflat guests of similar size.

Classes of Guests. In Figure 6, log k_{in} is plotted versus log K_a for each studied guest in order to differentiate the guests

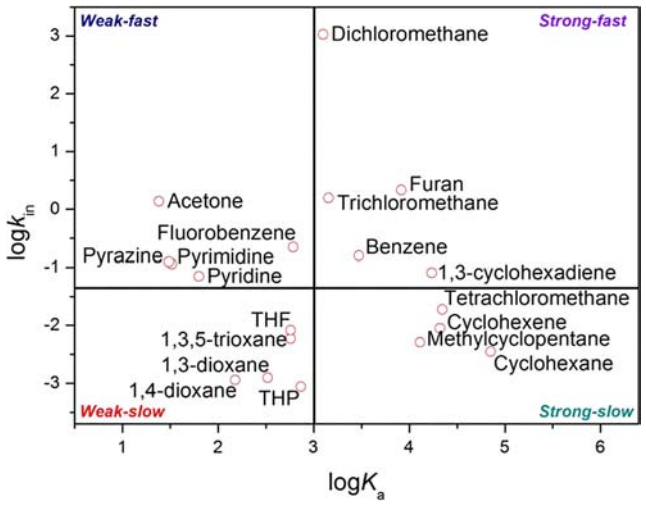

Figure 6. Quadrant plot of log k_{in} versus log K_a for each guest.

according to these two key parameters. It is possible to identify four types of guests: weak–slow, weak–fast, strong–slow, and strong–fast.

Many guest properties are responsible for the diversity of kinetic and thermodynamic parameters observed among different guests. The guest size is the most important factor in determining whether or not a molecule can be accommodated within the host's cavity; however, it does not seem to influence the strength of binding.

Size does, however, have a strong influence upon the uptake rate, with smaller guests entering the cavity faster than larger ones. Moreover, the shape of the guest strongly influences the uptake rate, with flat molecules being encapsulated more rapidly than similarly sized nonflat ones. Finally, the binding strength is clearly dependent on the hydrophobicity of the guest, as shown by the positive correlation between log K_a and log*P*.

Controlled Sequential Guest Uptake. The detailed understanding of the host–guest kinetics and thermodynamics for cage **1** gained during the course of this study allowed us to design an experiment in which three different guests, added simultaneously to a solution of host **1**, would be encapsulated sequentially (Scheme 2). This work complements a recent

Scheme 2. Sequential Formation of Acetone, Chloroform and 1,3,5-Trioxane Host–Guest Complexes following Simultaneous Addition of All Three Guests[a]

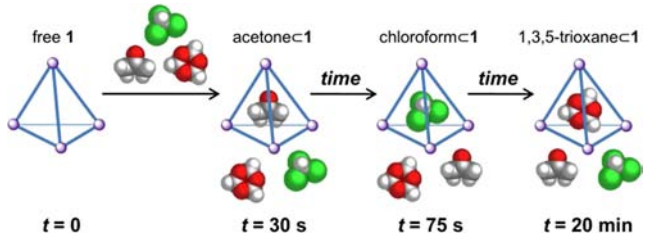

[a]Only the major host–guest complex (>80%) is shown for each step; moreover, the time elapsed after the start of the experiment is reported.

study in which affinity differentials between two hosts and five different anionic guests could be exploited to induce a chain-reaction anion exchange between hosts by adding first one anion and then another.[34]

The guests chosen for the experiment reported herein were acetone, chloroform, and 1,3,5-trioxane, which were selected on the basis of their K_a and k_{in} values. The experiment was designed so that acetone, the weakest guest, would be the first one to go into the host cavity. Chloroform would then displace acetone before being displaced by 1,3,5-trioxane. Indeed, NMR spectroscopy showed that consecutive displacement occurred exactly as anticipated (Figure 7). The guests' concentrations (acetone, chloroform, and 1,3,5-trioxane in a ratio of 170:24:485 relative to host **1**) were set to ensure that acetone would have the highest rate of uptake, followed by chloroform and 1,3,5-trioxane. At the same time, it was necessary to consider the thermodynamics of the system; therefore, these concentrations were chosen to ensure that the guest encapsulated second-fastest could displace the fastest guest as well as be displaced by the slowest guest.

As a further demonstration of how a system comprising cage **1** and a collection of different guests can be shown to express complex behavior, we extended the above sequence by taking advantage of the possibility of ejecting the guest pyridine through control of pH (Scheme 3). The initial state of the system consisted of a mixture of the three guests pyridine, acetone, and tetrahydrofuran (THF) in a ratio of 100:56:7 relative to host **1**. At neutral pH, predominantly pyridine was encapsulated by host **1** (degree of encapsulation 74%; Figure 8). Subsequent lowering of the pH resulted in protonation of the pyridine and consequently in release of pyridinium from the host.

dx.doi.org/10.1021/ja402084x | J. Am. Chem. Soc. 2013, 135, 7039–7046

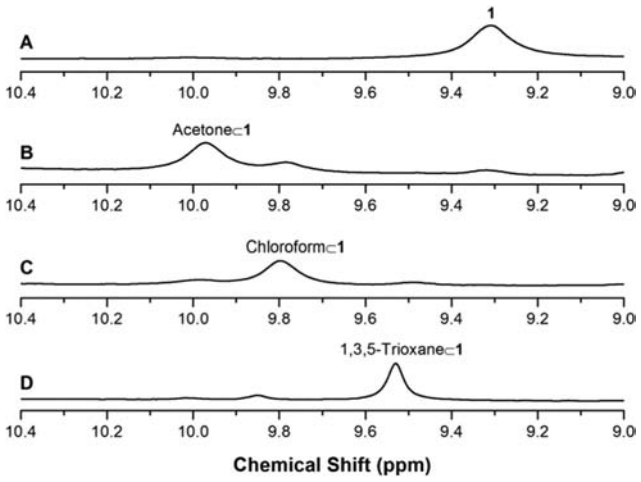

Figure 7. Stacked graph of NMR spectra (only the imine region is displayed) corresponding to the states of the sequential guest uptake shown in Scheme 2, going from (A) free host **1** before the simultaneous guest addition to (D) mostly 1,3,5-trioxane⊂**1** host–guest complex at the end of the experiment. Following addition of the guests, NMR spectra were acquired after (B) t = 30 s, (C) t = 75 s, and (D) t = 20 min. T = 298 K.

Scheme 3. pH-Controlled Switching between Pyridine, Acetone, and THF Host–Guest Complexes[a]

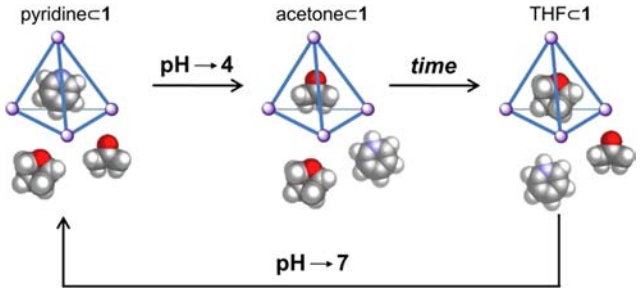

[a]Only the major host–guest complex is shown for each step.

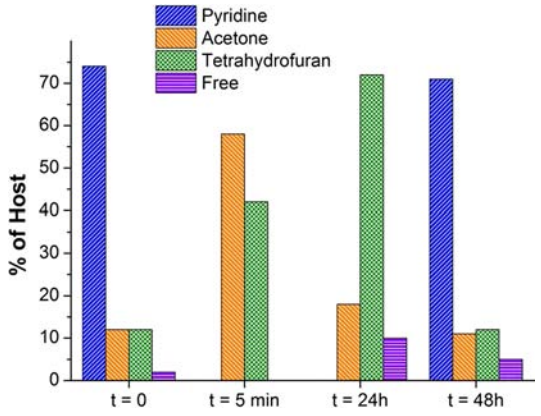

Figure 8. Composition of a reaction mixture containing host **1** and the guests pyridine, acetone, and THF to which deuterated trifluoroacetic acid was added at t = 0 and $NaHCO_3$ was added after 24 h: (A) t = 0; (B) t = 5 min; (C) t = 24 h (before addition of $NaHCO_3$); (D) t = 48 h (24 h after addition of $NaHCO_3$).

By ^{1}H NMR spectroscopy it was possible to monitor the ingress of acetone concomitant with the egress of pyridinium (Figure 8). That is, after 5 min nearly 60% of the cages encapsulated acetone. Further equilibration resulted in the release of acetone from the cage cavities in favor of encapsulation of THF, ultimately leading to 70% binding of THF at equilibrium (Figure 8). After the solution had re-equilibrated [i.e., after THF had become the major guest encapsulated by cage **1** (72%)], the pH was again raised, which resulted in the displacement of THF in favor of pyridine (Figure 8), thus cycling the system back to its original state (71% degree of binding for pyridine, which is equal to the initial value of 74% within the uncertainty of ^{1}H NMR integration).

CONCLUSIONS

On the basis of NMR studies in combination with principal component analysis, a quantitative understanding of the binding of a range of structurally different guests within capsule **1** was obtained. Different guest molecular properties were found to be strongly correlated to the observed strength and kinetics of binding. These quantitative insights allowed us to design and perform multiple guest-binding experiments in which their different binding strengths and uptake rates were exploited to control the order of encapsulation as a function of time. These sequential guest-binding series could be made reversible by inclusion of a pH-sensitive guest.

These results show how detailed physical-organic insights into individual binding events can be used to design complex, system-wide behavior. The time-dependent sequential uptake and release of specific guests might be used in similar systems to control the concentrations of specific reagents in a reaction mixture[8] or to release one reagent specifically as another is produced to displace it. Two or more such container molecules might even work in tandem, each with its own guest selectivity, allowing for complex sequences of uptake and release events to occur in response to chemical stimuli. Our study thus helps to demonstrate the utility of "simple" container molecules in achieving complex behavior within chemical systems.[4]

ASSOCIATED CONTENT

Supporting Information

Experimental procedures, NMR titration studies, K_a and k_{in} determination, equilibrium equation derivation, and sequential guest-uptake experiments. This material is available free of charge via the Internet at http://pubs.acs.org.

AUTHOR INFORMATION

Corresponding Author

m.m.j.smulders@utwente.nl; jrn34@cam.ac.uk

Present Address

[†]M.M.J.S.: Laboratory for Biomolecular Nanotechnology, MESA+ Institute for Nanotechnology, University of Twente, P.O. Box 217, 7500 AE Enschede, The Netherlands.

Author Contributions

[‡]M.M.J.S. and S.Z. contributed equally.

Notes

The authors declare no competing financial interest.

ACKNOWLEDGMENTS

This work was underwritten by the U.K. Engineering and Physical Sciences Research Council (EPSRC). M.M.J.S. acknowledges support from The Netherlands Organization for Scientific Research (NWO Rubicon Fellowship).

REFERENCES

(1) Lehn, J.-M. *Angew. Chem., Int. Ed. Engl.* **1988**, *27*, 89.
(2) Rybtchinski, B. *ACS Nano* **2011**, *5*, 6791.
(3) Gibb, B. C. *Nat. Chem.* **2011**, *3*, 3.
(4) Ludlow, R. F.; Otto, S. *Chem. Soc. Rev.* **2008**, *37*, 101.
(5) (a) Kindermann, M.; Stahl, I.; Reimold, M.; Pankau, W. M.; von Kiedrowski, G. *Angew. Chem., Int. Ed.* **2005**, *44*, 6750. (b) del Amo, V.; Philp, D. *Chem.—Eur. J.* **2010**, *16*, 13304. (c) Jiang, W.; Nowosinski, K.; Löw, N. L.; Dzyuba, E. V.; Klautzsch, F.; Schäfer, A.; Huuskonen, J.; Rissanen, K.; Schalley, C. A. *J. Am. Chem. Soc.* **2012**, *134*, 1860. (d) Hansen, S. W.; Stein, P. C.; Sørensen, A.; Share, A. I.; Witlicki, E. H.; Kongsted, J.; Flood, A. H.; Jeppesen, J. O. *J. Am. Chem. Soc.* **2012**, *134*, 3857. (e) Chung, M.-K.; White, P. S.; Lee, S. J.; Waters, M. L.; Gagné, M. R. *J. Am. Chem. Soc.* **2012**, *134*, 11415. (f) Chung, M.-K.; Lee, S. J.; Waters, M. L.; Gagné, M. R. *J. Am. Chem. Soc.* **2012**, *134*, 11430. (g) Jo, J.; Olasz, A.; Chen, C.-H.; Lee, D. *J. Am. Chem. Soc.* **2013**, *135*, 3620.
(6) (a) Pluth, M. D.; Bergman, R. G.; Raymond, K. N. *Acc. Chem. Res.* **2009**, *42*, 1650. (b) Kissel, P.; Erni, R.; Schweizer, W. B.; Rossell, M. D.; King, B. T.; Bauer, T.; Götzinger, S.; Schlüter, A. D.; Sakamoto, J. *Nat. Chem.* **2012**, *4*, 287. (c) Chakrabarty, R.; Mukherjee, P. S.; Stang, P. J. *Chem. Rev.* **2011**, *111*, 6810. (d) Ward, M. D. *Chem. Commun.* **2009**, 4487. (e) Albrecht, M.; Janser, I.; Frohlich, R. *Chem. Commun.* **2005**, 157. (f) Sun, Q.-F.; Iwasa, J.; Ogawa, D.; Ishido, Y.; Sato, S.; Ozeki, T.; Sei, Y.; Yamaguchi, K.; Fujita, M. *Science* **2010**, *328*, 1144. (g) Olenyuk, B.; Levin, M. D.; Whiteford, J. A.; Shield, J. E.; Stang, P. J. *J. Am. Chem. Soc.* **1999**, *121*, 10434. (h) Kumari, H.; Mossine, A. V.; Kline, S. R.; Dennis, C. L.; Fowler, D. A.; Teat, S. J.; Barnes, C. L.; Deakyne, C. A.; Atwood, J. L. *Angew. Chem., Int. Ed.* **2012**, *51*, 1452. (i) Smulders, M. M. J.; Riddell, I. A.; Browne, C.; Nitschke, J. R. *Chem. Soc. Rev.* **2013**, *42*, 1728. (j) Young, N. J.; Hay, B. P. *Chem. Commun.* **2013**, *49*, 1354. (k) Lusby, P. J.; Müller, P.; Pike, S. J.; Slawin, A. M. Z. *J. Am. Chem. Soc.* **2009**, *131*, 16398. (l) Mastalerz, M.; Schneider, M. W.; Oppel, I. M.; Presly, O. *Angew. Chem., Int. Ed.* **2011**, *50*, 1046. (m) Granzhan, A.; Schouwey, C.; Riis-Johannessen, T.; Scopelliti, R.; Severin, K. *J. Am. Chem. Soc.* **2011**, *133*, 7106.
(7) (a) Riddell, I. A.; Smulders, M. M. J.; Clegg, J. K.; Nitschke, J. R. *Chem. Commun.* **2011**, *47*, 457. (b) Custelcean, R.; Bosano, J.; Bonnesen, P. V.; Kertesz, V.; Hay, B. P. *Angew. Chem., Int. Ed.* **2009**, *48*, 4025. (c) Kishi, N.; Li, Z.; Yoza, K.; Akita, M.; Yoshizawa, M. *J. Am. Chem. Soc.* **2011**, *133*, 11438.
(8) Yoshizawa, M.; Klosterman, J. K.; Fujita, M. *Angew. Chem., Int. Ed.* **2009**, *48*, 3418.
(9) (a) Yoshizawa, M.; Tamura, M.; Fujita, M. *Science* **2006**, *312*, 251. (b) Natarajan, A.; Kaanumalle, L. S.; Jockusch, S.; Gibb, C. L. D.; Gibb, B. C.; Turro, N. J.; Ramamurthy, V. *J. Am. Chem. Soc.* **2007**, *129*, 4132.
(10) (a) Smulders, M. M. J.; Nitschke, J. R. *Chem. Sci.* **2012**, *3*, 785. (b) Leeland, J. W.; White, F. J.; Love, J. B. *J. Am. Chem. Soc.* **2011**, *133*, 7320. (c) Mal, P.; Breiner, B.; Rissanen, K.; Nitschke, J. R. *Science* **2009**, *324*, 1697.
(11) (a) Turega, S.; Whitehead, M.; Hall, B. R.; Meijer, A. J. H. M.; Hunter, C. A.; Ward, M. D. *Inorg. Chem.* **2013**, *52*, 1122. (b) García-Simón, C.; Garcia-Borràs, M.; Gómez, L.; Garcia-Bosch, I.; Osuna, S.; Swart, M.; Luis, J. M.; Rovira, C.; Almeida, M.; Imaz, I.; Maspoch, D.; Costas, M.; Ribas, X. *Chem.—Eur. J.* **2013**, *19*, 1445. (c) Custelcean, R.; Bonnesen, P. V.; Duncan, N. C.; Zhang, X.; Watson, L. A.; Van Berkel, G.; Parson, W. B.; Hay, B. P. *J. Am. Chem. Soc.* **2012**, *134*, 8525. (d) Kilbas, B.; Mirtschin, S.; Riis-Johannessen, T.; Scopelliti, R.; Severin, K. *Inorg. Chem.* **2012**, *51*, 5795. (e) Sun, Q.-F.; Sato, S.; Fujita, M. *Nat. Chem.* **2012**, *4*, 330. (f) Freye, S.; Hey, J.; Torras-Galán, A.; Stalke, D.; Herbst-Irmer, R.; John, M.; Clever, G. H. *Angew. Chem., Int. Ed.* **2012**, *51*, 2191. (g) Wang, Q.-Q.; Day, V. W.; Bowman-James, K. *Angew. Chem., Int. Ed.* **2012**, *51*, 2119. (h) Paul, L. E. H.; Therrien, B.; Furrer, J. *Inorg. Chem.* **2012**, *51*, 1057. (i) Mishra, A.; Vajpayee, V.; Kim, H.; Lee, M. H.; Jung, H.; Wang, M.; Stang, P. J.; Chi, K.-W. *Dalton Trans.* **2012**, *41*, 1195. (j) Pitto-Barry, A.; Barry, N. P. E.; Zava, O.; Deschenaux, R.; Dyson, P. J.; Therrien, B. *Chem.—Eur. J.* **2011**, *17*, 1966. (k) Ballester, P. *Chem. Soc. Rev.* **2010**, *39*, 3810. (l) Steed, J. W. *Chem. Soc. Rev.* **2009**, *38*, 506. (m) Sawada, T.; Fujita, M. *J. Am. Chem. Soc.* **2010**, *132*, 7194. (n) Leung, D. H.; Bergman, R. G.; Raymond, K. N. *J. Am. Chem. Soc.* **2006**, *128*, 9781. (o) Leung, D. H.; Bergman, R. G.; Raymond, K. N. *J. Am. Chem. Soc.* **2008**, *130*, 2798. (p) Clegg, J. K.; Cremers, J.; Hogben, A. J.; Breiner, B.; Smulders, M. M. J.; Thoburn, J. D.; Nitschke, J. R. *Chem. Sci.* **2013**, *4*, 68. (q) Samanta, D.; Mukherjee, S.; Patil, Y. P.; Mukherjee, P. S. *Chem.—Eur. J.* **2012**, *18*, 12322.
(12) Davis, A. V.; Fiedler, D.; Seeber, G.; Zahl, A.; van Eldik, R.; Raymond, K. N. *J. Am. Chem. Soc.* **2006**, *128*, 1324.
(13) Jiang, W.; Ajami, D.; Rebek, J., Jr. *J. Am. Chem. Soc.* **2012**, *134*, 8070.
(14) Mal, P.; Schultz, D.; Beyeh, K.; Rissanen, K.; Nitschke, J. R. *Angew. Chem., Int. Ed.* **2008**, *47*, 8297.
(15) Ronson, T. K.; Giri, C.; Beyeh, N. K.; Minkkinen, A.; Topić, F.; Holstein, J. J.; Rissanen, K.; Nitschke, J. R. *Chem.—Eur. J.* **2013**, *19*, 3374.
(16) Biros, S. M.; Bergman, R. G.; Raymond, K. N. *J. Am. Chem. Soc.* **2007**, *129*, 12094.
(17) Zarra, S.; Smulders, M. M. J.; Lefebvre, Q.; Clegg, J. K.; Nitschke, J. R. *Angew. Chem., Int. Ed.* **2012**, *51*, 6882.
(18) Jurs, P. C.; Bakken, G. A.; McClelland, H. E. *Chem. Rev.* **2000**, *100*, 2649.
(19) (a) Folmer-Andersen, J. F.; Kitamura, M.; Anslyn, E. V. *J. Am. Chem. Soc.* **2006**, *128*, 5652. (b) Buryak, A.; Severin, K. *J. Am. Chem. Soc.* **2005**, *127*, 3700.
(20) Hristova, Y. R.; Smulders, M. M. J.; Clegg, J. K.; Breiner, B.; Nitschke, J. R. *Chem. Sci.* **2011**, *2*, 638.
(21) Abraham, M. H.; Le, J. *J. Pharm. Sci.* **1999**, *88*, 868.
(22) To prevent the formation of a second, organic phase into which the second hydrophobic guest could be extracted, the amount of added benzene was limited to 5.0 μL per 0.5 mL of water. See the Supporting Information for details.
(23) Chapman, N. B.; Shorter, J. *Correlation Analysis in Chemistry: Recent Advances*; Plenum Press: New York, 1978.
(24) Consonni, V.; Todeschini, R. *Handbook of Molecular Descriptors*; Wiley-VCH: Weinheim, Germany, 2000.
(25) (a) Leach, A. R.; Gillet, V. J. In *An Introduction to Chemoinformatics*; Springer: Dordrecht, The Netherlands, 2007; p 69. (b) Alunni, S.; Clementi, S.; Edlund, U.; Johnels, D.; Hellberg, S.; Sjöström, M.; Wold, S. *Acta Chem. Scand. B* **1983**, *37*, 47.
(26) *CRC Handbook of Chemistry and Physics*, 93rd ed.; Haynes, W. M., Ed.; CRC Press: Boca Raton, FL, 2012.
(27) Davis, A. V.; Raymond, K. N. *J. Am. Chem. Soc.* **2005**, *127*, 7912.
(28) We previously presented data supporting a through-face mechanism for guest exchange into host **1** (ref 17). The present study confirmed this mechanism, since the alternative slow deligation mechanism (ref 11p) could not explain the high guest-uptake rate constants reported herein.
(29) Lu, J.; Ma, D.; Hu, J.; Tang, W.; Zhu, D. *J. Chem. Soc., Dalton Trans.* **1998**, 2267.
(30) Pastor, A.; Martínez-Viviente, E. *Coord. Chem. Rev.* **2008**, *252*, 2314.
(31) Todeschini, R.; Consonni, V. In *Handbook of Chemoinformatics*; Gasteiger, J., Ed.; Wiley-VCH: Weinheim, Germany, 2008; p 1004.
(32) (a) Rudnick, J.; Gaspari, G. *J. Phys. A: Math. Gen.* **1986**, *19*, L191. (b) Rudnick, J.; Gaspari, G. *Science* **1987**, *237*, 384. (c) Baumgärtner, A. *J. Chem. Phys.* **1993**, *98*, 7496.
(33) (a) Pearson, K. *Philos. Trans. R. Soc. London, Ser. A* **1895**, *186*, 343. (b) Rodgers, J. L.; Nicewander, W. A. *Am. Stat.* **1988**, *42*, 59.
(34) Ma, S.; Smulders, M. M. J.; Hristova, Y. R.; Clegg, J. K.; Ronson, T. K.; Zarra, S.; Nitschke, J. R. *J. Am. Chem. Soc.* **2013**, DOI: 10.1021/ja311882h.